Sensor and Simulation Notes

Note 509

February 2006

Focal Waveform of a Prolate-Spheroidal IRA

Carl E. Baum
University of New Mexico
Department of Electrical and Computer Engineering
Albuquerque New Mexico 87131

Abstract

This paper develops some analytic approximations for the focal waveform produced at the second focus of a prolate-spheroidal reflector due to a TEM wave launched from the first focus. This is extended to consider the spot size of the peak field near the second focus.

`

This work was sponsored in part by the Air Force Office of Scientific Research. ***R1***

1. Introduction

Two previous papers [9, 10] have discussed the basic concept of using one or more prolate spheroidal reflectors to focus a fast-transient electromagnetic pulse on some targets of interest. Another paper [11] has shown that an inhomogeneous spherical TEM wave launched on guiding conical conductors from one focus is converted by a double stereographic transformation to a second (reflected) inhomogeneous spherical TEM wave propagating toward the second focus. Both waves have the same temporal waveforms before other scattering (from feed arms, etc.) can reach the observer.

The present paper is concerned with analytic calculations of the waveform at the second focus. For this purpose let us consider the geometry in Fig. 1.1. Let there be two thin perfectly conducting cone wave launchers with electrical centers lying in the *xz* plane. With respect to the negative *z* axis they are oriented at

$$\theta_1 = \theta_c \tag{1.1}$$

in the wave-launching spherical system (r_1 , θ_1 , ϕ_1). These are related to cylindrical (Ψ_1 , ϕ_1 , z_1) and Cartesian (*x*, *y*, *z*) coordinates as

$$\begin{aligned} \Psi_1 &= r_1 \sin(\theta_1) \quad , \quad z = -z_0 - r_1 \cos(\theta_1) \\ x &= \Psi_1 \cos(\phi_1) \quad , \quad y = -\Psi_1 \sin(\phi_1) \\ \phi_1 &= -\phi \quad , \quad \Psi = \Psi_1 \\ z_1 &= -z + z_0 \end{aligned} \tag{1.2}$$

The prolate spheroid is described by

$$\begin{aligned} \left[\frac{\Psi}{b}\right]^2 + \left[\frac{z}{a}\right]^2 &= 1 \\ z_0 &= \left[a^2 - b^2\right]^{1/2} \end{aligned} \tag{1.3}$$

The thin-cone electrical centers are described by the angle θ_c with

$$\begin{aligned} \Psi_c &= r_1 \sin(\theta_c) \\ z_c &= -z_0 - r_1 \cos(\theta_c) \end{aligned} \tag{1.4}$$

At the reflector we have (subscript *p*)

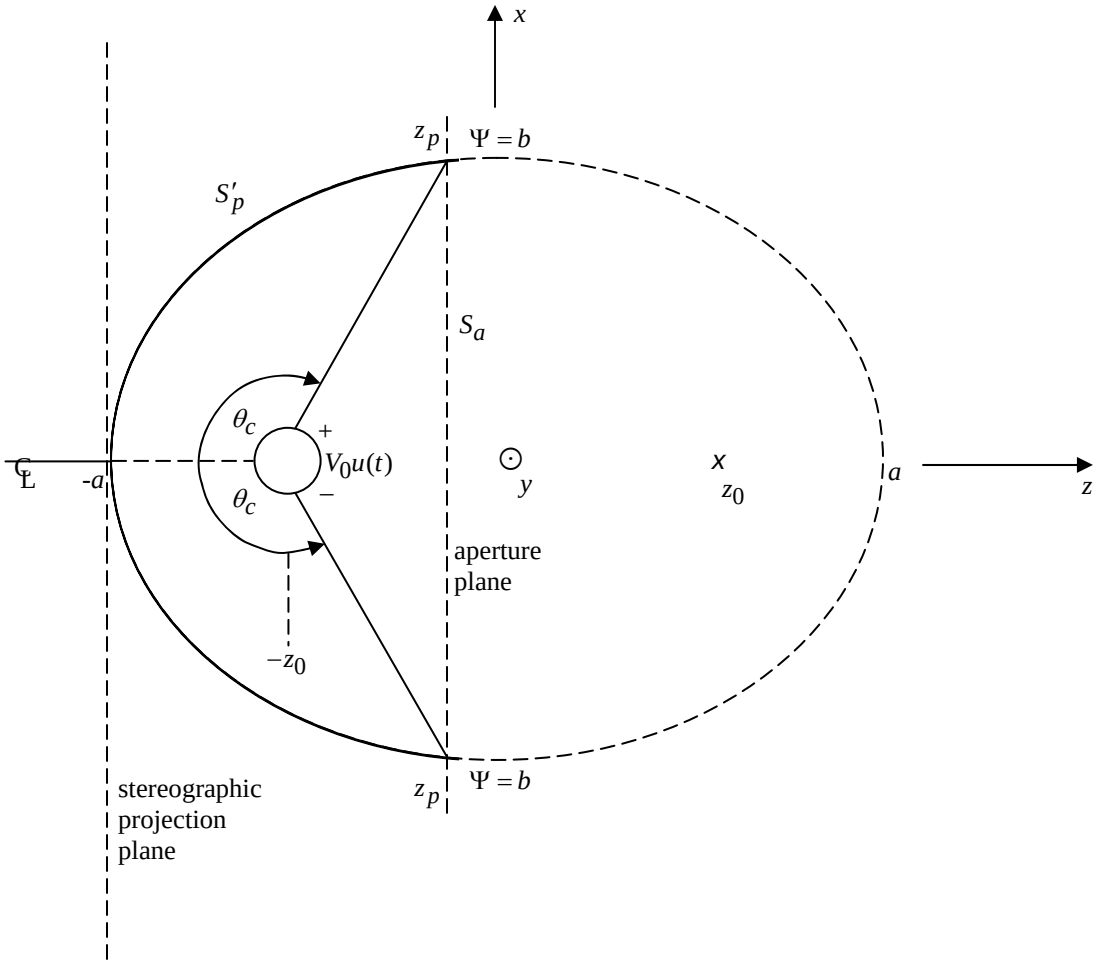

Fig. 1.1 Wave Launcher in Prolate-Spheroidal Reflector

$$
\begin{aligned}
& z_p = -z_0 - \Psi_p \cot(\theta_c) \\
& \left[\frac{\left[-z_0 - z_p\right]}{b}\tan(\theta_c)\right]^2 + \left[\frac{z_p}{a}\right]^2 = 1 \\
& \tan^2(\theta_c) = \left[\frac{b}{z_0 + z_p}\right]^2\left[1 - \left[\frac{z_p}{a}\right]^2\right]
\end{aligned}
\tag{1.5}
$$

Given θ_c one can solve for z_p and Ψ_p. One can also specify z_p and compute Ψ_p and θ_c.

As a special case one may choose the symmetry plane for which

$$z_p = z = 0 \tag{1.6}$$

This simplifies the equations to

$$
\begin{aligned}
& \Psi_p = b \quad , \quad r_{1_p} = a \\
& \sin(\theta_c) = \sin(\pi - \theta_c) = \frac{b}{a} \\
& \frac{\pi}{2} < \theta_c < \pi
\end{aligned}
\tag{1.7}
$$

For the present let us truncate the reflector at the $z = z_p$ plane. The portion used is S_p', to the left. This is consistent with the traditional truncation of paraboloidal reflector impulse radiating antennas (IRAs). More sophisticated truncation contours can be considered, but are beyond the scope of this paper. For later use the truncation plane will be taken as an aperture plane. The portion of this plane inside the prolate sphere is designated S_a. It is this surface which will be used for integrating over the reflected TEM wave to find the fields at the second focus, $\vec{r}_0$.

2. Prepulse

The stereographic projections in [11] can be used to calculate the fields. Let wave 1 have the form

$$\begin{aligned}
&\vec{E}_1 = -r_1^{-1}\nabla_{\theta_1,\phi_1}\ V_1(\theta_1,\ \phi_1)\ u\left(t - \frac{r_1}{c}\right)\\
&\nabla_{\theta_1,\phi_1} = \vec{1}_{\theta_1}\frac{\partial}{\partial\theta_1} + \vec{1}_{\phi_1}\frac{1}{\sin(\theta_1)}\frac{\partial}{\partial\phi_1}\\
&\nabla^2_{\theta_1,\phi_1}\ V_1(\theta_1,\ \phi_1) = 0\\
&\nabla^2_{\theta_1,\phi_1} = \frac{1}{\sin(\theta_1)}\frac{\partial}{\partial\theta_1}\sin(\theta_1)\frac{\partial}{\partial\theta_1} + \frac{1}{\sin^2(\theta_1)}\frac{\partial^2}{\partial\phi^2}\\
&c = \left[\mu\varepsilon\right]^{-1/2} = \text{wave speed in medium}
\end{aligned} \tag{2.1}$$

Let the wave have $V_1 = \pm V_0$ on the two cones.

The stereographic projection of this wave is

$$\Psi_0 = 2\left[a - z_0\right]\tan\left(\frac{\theta_1}{2}\right),\ \ \phi_0 = -\phi_1 = -\phi \tag{2.2}$$

The electrical center of the thin wire on this projection plane is

$$\begin{aligned}
&\Psi_{c0} = 2\left[a - z_0\right]\tan\left(\frac{\theta_c}{2}\right),\ \ \phi_{c0} = 0,\pi\\
&r_{w0} = \text{radius of thin wire on projection plane}
\end{aligned} \tag{2.3}$$

For the two thin wires we have the well-known solution [1, 5]

$$\begin{aligned}
&V(x_0, y_0) = V_0\ \text{arccosh}^{-1}\left(\frac{\Psi_{c0}}{r_{w0}}\right)\frac{1}{2}\ell\text{n}\left(\frac{\left[\frac{y_0}{\Psi_{c0}}\right]^2 + \left[1+\frac{x_0}{\Psi_{c0}}\right]^2}{\left[\frac{y_0}{\Psi_{c0}}\right]^2 + \left[1-\frac{x_0}{\Psi_{c0}}\right]^2}\right)\\
&\text{arccosh}\left(\frac{\Psi_{c0}}{r_{w0}}\right) \simeq \ell\text{n}\left(2\frac{\Psi_{c0}}{r_{w0}}\right)
\end{aligned} \tag{2.4}$$

From this we have

$$
\begin{aligned}
Z_c &= Z_0\, f_g \equiv \text{characteristic impedance} \\
Z_0 &= \left[\frac{\mu}{\varepsilon}\right]^{1/2} \equiv \text{wave impedance of medium} \\
f_g &= \frac{1}{\pi}\operatorname{arccosh}\left(\frac{\Psi_{c0}}{r_{w0}}\right) \simeq \frac{1}{\pi}\ell\mathrm{n}\left(2\frac{\Psi_{c0}}{r_{w0}}\right)
\end{aligned}
\tag{2.5}
$$

It is often convenient to specify Z_c (around 400 Ω), and from this determine the various transmission-line parameters. In this case we have

$$
f_g \simeq \frac{400}{377} \simeq 1.06\ ,\ \frac{\Psi_{c0}}{r_{w0}} \simeq 14 \tag{2.6}
$$

for typical numbers.

Converting (2.4) to (θ_1 , ϕ_1) coordinates we have

$$
\begin{aligned}
V_1(\theta_1\ ,\ \phi_1) &= \frac{V_0}{2}\operatorname{arccosh}^{-1}\left(\frac{\Psi_{c0}}{r_{w0}}\right)\ell\mathrm{n}\left(\frac{\left[\frac{\Psi_{c0}}{r_{w0}}\right]^2 + 2\frac{\Psi_0}{\Psi_{c0}}\cos(\phi_1)+1}{\left[\frac{\Psi_0}{\Psi_{c0}}\right]^2 - 2\frac{\Psi_0}{\Psi_{c0}}\cos(\phi_1)+1}\right) \\
\Psi_0 &= 2\left[a - z_0\right]\tan\left(\frac{\theta_1}{2}\right)
\end{aligned}
\tag{2.7}
$$

for the potential in wave 1. The gradient in (2.1) then gives the electric field. A special case has

$$
\begin{aligned}
\phi_1 &= \pm\pi/2 \\
V_1 &= 0
\end{aligned}
\tag{2.8}
$$

which is a symmetry plane (the $x = 0$ plane). Another symmetry plane (the $y = 0$ plane) has

$$
\begin{aligned}
&\phi_1 = 0 \quad (\text{for } \Psi_0 = +x) \\
&V_1(\theta_1\ ,\ \phi_1) = V_0\operatorname{arccosh}^{-1}\left(\frac{\Psi_{c0}}{r_{w0}}\right)\ell\mathrm{n}\left(\frac{\frac{\Psi_0}{\Psi_{c0}} + 1}{\frac{\Psi_0}{\Psi_{c0}} - 1}\right)
\end{aligned}
$$

$$= V_0 \operatorname{arccosh}^{-1}\left(\frac{\Psi_{c0}}{r_{w0}}\right) \ell n\left(\frac{1 + \frac{\Psi_{c0}}{\Psi_0}}{1 - \frac{\Psi_{c0}}{\Psi_0}}\right) = V_0 \operatorname{arccosh}^{-1}\left(\frac{\Psi_{c0}}{r_{w0}}\right)\left[2\frac{\Psi_{c0}}{\Psi_0} + \mathrm{O}\left(\left[\frac{\Psi_{c0}}{\Psi_0}\right]^2\right)\right] \tag{2.9}$$
$$= V_0 \operatorname{arccosh}^{-1}\left(\frac{\Psi_{c0}}{r_{w0}}\right)\left[\frac{\Psi_{c0}}{a - z_0} \cot\left(\frac{\theta_1}{2}\right) + \cdots\right]$$

For θ_1 near π this is

$$V_1(\theta_1, \phi_1) = V_0 \operatorname{arccosh}^{-1}\left(\frac{\Psi_{c0}}{r_{w0}}\right)\left[\frac{\Psi_{c0}}{a - z_0} \frac{\pi - \theta_1}{2} + \cdots\right], \quad \Psi_{c0} = 2\left[a - z_0\right]\tan\left(\frac{\theta_c}{2}\right)$$
$$V_1(\theta_1, \phi_1) = V_0 \operatorname{arccosh}^{-1}\left(\frac{\Psi_{c0}}{r_{w0}}\right)\left[\tan\left(\frac{\theta_c}{2}\right)\left[\pi - \theta_1\right] + \cdots\right], \quad \pi f_g = \operatorname{arccosh}\left(\frac{\Psi_{c0}}{r_{w0}}\right) \simeq \ell \mathrm{n}\left(2\frac{\Psi_{c0}}{r_{w0}}\right) \tag{2.10}$$

From (2.1) we have at the second focus

$$r_1 = 2z_0$$
$$\vec{E}_1 = -E_p u\left(t - \frac{2z_0}{c}\right)\vec{1}_x \tag{2.11}$$
$$E_p = \frac{V_0}{4z_0} \operatorname{arccosh}^{-1}\left(\frac{\Psi_{c0}}{r_{w0}}\right)\frac{\Psi_{c0}}{a - z_0} \simeq \frac{V_0}{2z_0 \pi f_g}\tan\left(\frac{\theta_c}{2}\right)$$

This is the prepulse orientation and magnitude (for step excitation). It lasts for a time [11]

$$\Delta t_p = \frac{2\left[a - z_0\right]}{c} = \frac{2}{c}\left[a - \left[a^2 - b^2\right]^{1/2}\right] = 2\frac{a}{c}\left[1 - \left[1 - \left[\frac{b}{a}\right]^2\right]^{1/2}\right] \tag{2.12}$$

after which the reflector signal arrives at the second focus.

For the special case as in (1.6) and (1.7) for which the launcher intersects the reflector at the z = 0 symmetry plane we have

$$\tan\left(\frac{\theta_c}{2}\right) = \frac{1 - \cos(\theta_c)}{\sin(\theta_c)} = \frac{a}{b}\left[1 + \left[1 - \left[\frac{b}{a}\right]^2\right]^{1/2}\right] = \frac{1}{b}\left[a + z_0\right] \tag{2.13}$$
$$E_p \simeq \frac{V_0}{2\pi f_g} \frac{a + z_0}{b\, z_0}$$
$$E_p \Delta t_p \simeq \frac{V_0}{\pi f_g} \frac{b}{c\, z_0} \text{ (time integral or “area” of prepulse)}$$

3. Fields on Aperture Plane

Now we consider the wave heading from the reflector toward the second focus. There is no set of conical conductors guiding the wave there. So we consider this second spherical TEM wave [11] on the aperture plane, which we can use in turn to find the fields at $\vec{r}_0$ (and other positions as well). For present purposes we take the aperture plane as $z = z_p$, as in Fig. 1.1. The reflected wave illuminates S_a, a disk of radius Ψ_p.

Note that the reflector is truncated at the aperture plane. This is because the field from the wavelauncher reverses sign for the wave on the "other side" of the launching conductors. This is the same truncation used for typical reflector IRAs, based on a self-reciprocal geometry [12]. There are more sophisticated (nonplanar) truncation geometries which may be considered in the future.

In [11] the reflected wave was related to the first wave by a double stereographic transformation. They are equal (except for a minus sign) on the stereographic projection plane ($z = -a$) for which

$$
\begin{aligned}
&V_2(\Psi_0\,,\ \phi_0) = -V_1(\Psi_0\,,\ \phi_0) \\
&(\Psi_0\,,\ \phi_0) \equiv \text{cylindrical coordinates on projection plane} \\
&\Psi_0 = 2[a - z_0]\tan\left(\frac{\theta_1}{2}\right) = 2[a + z_0]\tan\left(\frac{\theta_2}{2}\right) \\
&\phi_0 = -\phi_1 = -\phi_2
\end{aligned}
\tag{3.1}
$$

The second TEM wave takes the form

$$
\vec{E}_2 = -\vec{r}_2^{\,-1}\,\nabla_{\theta_2,\phi_2} V_2(\theta_2, \phi_2)\,\mu\left(t + \frac{r_2}{\mathrm{c}} - 2\frac{a}{c}\right) \tag{3.2}
$$

Note the factor giving an incoming (on $\vec{r}_0$) step-function wave.

For the aperture integral we need the tangential electric field on S_a. First we have

$$
\begin{aligned}
&V_2(\theta_2\,,\ \phi_2) = -\frac{V_0}{2}\,\mathrm{arccosh}^{-1}\left(\frac{\Psi_{c0}}{r_{w0}}\right)\ell\mathrm{n}\left(\frac{\left[\frac{\Psi_0}{\Psi_{c0}}\right]^2 + 2\frac{\Psi_0}{\Psi_{c0}}\cos(\phi_1) + 1}{\left[\frac{\Psi_0}{\Psi_{c0}}\right]^2 - 2\frac{\Psi_0}{\Psi_{c0}}\cos(\phi_1) + 1}\right) \\
&\Psi_0 = 2[a + z_0]\tan\left(\frac{\theta_2}{2}\right)\ ,\quad \Psi_{c0} = 2[a - z_0]\tan\left(\frac{\theta_c}{2}\right)
\end{aligned}
\tag{3.3}
$$

For θ_2 near zero we have

$$\begin{aligned} V_2(\theta_2\,,\,\phi_2) &= -\frac{V_0}{2}\operatorname{arccosh}^{-1}\left(\frac{\Psi_{c0}}{r_{w0}}\right)\left[4\frac{\Psi_0}{\Psi_{c0}}\cos(\phi_1) + \cdots\right] \\ &= -V_0\operatorname{arccosh}^{-1}\left(\frac{\Psi_{c0}}{r_{w0}}\right)\left[2\frac{a+z_0}{a-z_0}\cot\left(\frac{\theta_c}{2}\right)\frac{\theta_2}{2}\cos(\phi_1) + \cdots\right] \\ \operatorname{arccosh}^{-1}&\left(\frac{\Psi_{c0}}{r_{w0}}\right) \simeq \pi\, f_g \\ \vec{E}_2 &\simeq \frac{V_0}{r_2\pi\, f_g}\frac{a+z_0}{a-z_0}\cot\left(\frac{\theta_c}{2}\right)u\left(t + \frac{r_2}{c} - \frac{2a}{c}\right)\vec{1}_x \end{aligned} \tag{3.4}$$

Comparing this to the prepulse amplitude in (2.11) we have (θ_2 near 0)

$$\vec{E}_2 \simeq E_p\frac{2z_0}{r_2}\frac{a+z_0}{a-z_0}\cot^2\left(\frac{\theta_c}{2}\right)\vec{1}_x\,u\left(t + \frac{r_2}{c} - 2\frac{a}{c}\right) \tag{3.5}$$

For the special case (as in (2.13)) that the launcher intersects the reflector at the $z = 0$ symmetry plane we have (for θ_2 near zero)

$$\begin{aligned} \vec{E}_2 &\simeq \frac{V_0}{\pi f_g}\frac{z_0}{r_2}\frac{b}{a-z_0}u\left(t + \frac{r_2}{c} - 2\frac{a}{c}\right)\vec{1}_x \simeq E_p\frac{2z_0}{r_2}\frac{b^2}{[a-z_0][a+z_0]}u\left(t + \frac{r_2}{c} - 2\frac{a}{c}\right)\vec{1}_x \\ &= E_p\frac{2z_0}{r_2}u\left(t + \frac{r_2}{c} - 2\frac{a}{c}\right) \end{aligned} \tag{3.6}$$

a fairly simple result.

At the center of the aperture plane we have

$$\begin{aligned} r_2 &= z_0 - z_p\,,\ \vec{E}_2 \simeq E_{a0}\,u\left(t + \frac{z_0 - z_p}{c} - 2\frac{a}{c}\right)\vec{1}_x \\ E_{a0} &= \frac{V_0}{\pi f_g}\frac{1}{z_0 - z_p}\frac{a+z_0}{a-z_0}\cot\left(\frac{\theta_c}{2}\right) \\ &\simeq E_p\frac{2\,z_0}{z_0 - z_p}\frac{a+z_0}{a-z_0}\cot^2\left(\frac{\theta_c}{2}\right) \end{aligned} \tag{3.7}$$

For $z_p = 0$ this reduces to

$$E_{a0} = 2\,E_p \tag{3.8}$$

Wave number 2 is focused on $\vec{r}_0$. Without guiding conductors (3.5) cannot hold all the way as $r_2 \to 0$. So we are considering the fields on S_a for later integration. On the center of S_a we have the electric field E_0 polarized in the $\vec{1}_x$ direction.

In IRA-related calculations [5, 6] it has been seen that, for circular apertures, the field at the center is an important parameter. The boresight radiated field can be found by integrating the TEM field over the aperture, or by integrating a uniform field of the center value (including polarization) over the same circular aperture. Seen another way, one can expand the field in cylindrical coordinates and note that terms with $\cos(m\phi)$ and $\sin(m\phi)$ for $m \geq 2$ integrate to zero (for observation field points on the *z* axis). (There is no *m*= 0 term.) This is basically a symmetry result.

Similarly here, let us consider a uniform field on the $(\Psi_0\,,\ \phi_0)$ projection plane. This corresponds to a potential function

$$V_2' \ = \ -E_0 x_0 \ = \ -E_0 \Psi_0 \cos(\phi_0) \tag{3.9}$$

for a uniform field E_0 polarized in the *x* direction. Matching this field to the second wave at

$$\begin{aligned} r_2 \ &= \ a \ + \ z_0 \ \text{(center of projection plane)} \\ \vec{E}_2 \ &= \ E_0 \, u\left(t \ - \ \frac{z_0 - a}{c} \right) \vec{1}_x \\ E_0 \ &\simeq \ \frac{V_0}{\pi f_g} \frac{1}{a - z_0} \cot\left(\frac{\theta_c}{2} \right) \\ &\simeq \ E_p \frac{2 z_0}{a - z_0} \cot^2\left(\frac{\theta_c}{2} \right) \end{aligned} \tag{3.10}$$

For $z_p = 0$ this becomes

$$E_0 \ \simeq \ E_p \frac{2 z_0}{a + z_0} \ \simeq \ \frac{V_0}{\pi f_g b} \tag{3.11}$$

Now convert V_2' on the projection plane to $(\theta_2\,,\ \phi_2)$ coordinates as

$$V_2' \ = \ -E_0 2\left[a + z_0 \right] \tan\left(\frac{\theta_2}{2} \right) \cos(\phi_2) \tag{3.12}$$

giving an electric field

$$\begin{aligned}\vec{E}_2 &= E_0\frac{a+z_0}{r_2}\left[\sec^2\left(\frac{\theta_2}{2}\right)\cos(\theta_2)\,\vec{1}_{\theta_2}-2\tan\left(\frac{\theta_2}{2}\right)\frac{\sin(\phi_2)}{\sin(\theta_2)}\vec{1}_{\phi_2}\right]u\left(t+\frac{r_2}{c}-2\frac{a}{c}\right)\\ &= E_0\frac{a+z_0}{r_2}\left[\frac{2\cos(\phi_2)}{1+\cos(\theta_2)}\,\vec{1}_{\theta_2}-\frac{2\sin(\phi_2)}{1+\cos(\theta_2)}\,\vec{1}_{\phi_2}\right]u\left(t+\frac{r_2}{c}-2\frac{a}{c}\right)\end{aligned} \tag{3.13}$$

On the aperture plane we have

$$\begin{aligned} r_2 &= \left[\Psi^2+\left[z_0-z_p\right]^2\right]^{1/2}\\ \cos(\theta_2) &= \frac{z_0-z_p}{r_2}\\ r_2\left[1+\cos(\theta_2)\right] &= r_2+z_0-z_p\\ \phi &= -\phi_2 \quad , \quad \vec{1}_\phi = -\vec{1}_{\phi_2}\\ \vec{1}_{\theta_2}\cdot\vec{1}_\Psi &= \cos(\theta_2)\end{aligned} \tag{3.14}$$

The tangential electric field is then

$$\begin{aligned}\vec{E}_{2t} = 2E_0\frac{a+z_0}{r_2+z_0\,z_p}&\left[\frac{z_0-z_p}{r_2}\cos(\phi)\,\vec{1}_\Psi-\sin(\phi)\,\vec{1}_\phi\right]\\ &u\left(t+\frac{r_2}{c}-2\frac{a}{c}\right)\end{aligned} \tag{3.15}$$

Converting to Cartesian coordinates we need only the *x* component (due to symmetry) as

$$\begin{aligned}\vec{1}_\Psi\cdot\vec{1}_x &= \cos(\phi) = \vec{1}_\phi\cdot\vec{1}_y = -\sin(\phi)\\ E'_{2x} &= 2E_0\frac{a+z_0}{r_2+z_0-z_p}\left[\frac{z_0-z_p}{r_2}\cos^2(\phi)+\sin^2(\phi)\right]\\ E_{2x} &= E'_{2x}\,u\left(t+\frac{r_2}{c}-2\frac{a}{c}\right)\end{aligned} \tag{3.16}$$

4. Fields at Second Focus

We are now in a position to evaluate the fields at $\vec{r}_0$ by integrals over the fields on S_a. A previous paper [2] has developed the formulae. From [2 (3.3)] we have (in time domain for step excitation)

$$\begin{aligned}
&\vec{E}_f = E_{fx}\vec{1}_x \quad , \quad E_{fx} = E_\delta\,\delta\left(t - 2\frac{a}{c}\right) + E_s\,u\left(t - 2\frac{a}{c}\right) \\
&E_\delta = \frac{1}{2\pi c}\int_{S_a}\frac{z_0 - z_p}{r_2^e}E'_{2x}\,ds \quad , \quad E_s = \frac{1}{2\pi}\int_{S_a}\frac{z_0 - z_p}{r_2^3}E'_{2x}\,ds \\
&r_2 = \left[\left[z_0 - z_p\right]^2 + \Psi^2\right]^{1/2}
\end{aligned} \tag{4.1}$$

Using cylindrical coordinates on S_a we can evaluate the integrals. Considering first the ϕ variable we have

$$\begin{aligned}
E_\delta &= \frac{E_0}{\pi c}\int_0^{\Psi_p}\int_0^{2\pi}\frac{z_0 - z_r}{r_2^2}\frac{a + z_0}{r_2 + z_0 - z_p}\left[\frac{z_0 - z_p}{r_2}\cos^2(\phi) + \sin^2(\phi)\right]\Psi\,d\phi\,d\Psi \\
&= \frac{E_0}{c}\int_0^{\Psi_p}\frac{z_0 - z_p}{r_2^2}\frac{a + z_0}{r_2 + z_0 - z_p}\left[\frac{z_0 - z_p}{r_2} + 1\right]\Psi\,d\Psi \\
&= \frac{E_0}{c}\left[z_0 - z_p\right]\left[a + z_0\right]\int_0^{\Psi_p}\frac{\Psi}{r_2^3}d\Psi \\
E_s &= \frac{E_0}{\pi}\int_0^{\Psi_p}\int_0^{2\pi}\frac{z_0 - z_p}{r_2^3}\frac{a + z_0}{r_2 + z_0 - z_p}\left[\frac{z_0 - z_p}{r_2}\cos^2(\phi) + \sin^2(\phi)\right]\Psi\,d\phi\,d\Psi \\
&= E_0\int_0^{\Psi_p}\frac{z_0 - z_p}{r_2^3}\frac{a + z_0}{r_2 + z_0 - z_p}\left[\frac{z_0 - z_p}{r_2} + 1\right]\Psi\,d\Psi \\
&= E_0\left[z_0 - z_p\right]\left[a + z_0\right]\int_0^{\Psi_p}\frac{\Psi}{r_2^4}d\Psi
\end{aligned} \tag{4.2}$$

Next we have

$$\begin{aligned}
&r_2 = \left[\left[z_0 - z_p\right]^2 + \Psi^2\right]^{1/2} \quad , \quad \upsilon \equiv \Psi^2 + \left[z_0 - z_p\right]^2 \,,\; d\upsilon = 2\Psi\,d\Psi \\
&E_\delta = \frac{E_0}{2c}\left[z_0 - z_p\right]\left[a + z_0\right]\int_{\left[z_0 - z_p\right]^2}^{\Psi_p^2 + \left[z_0 - z_p\right]^2}\upsilon^{-3/2}d\upsilon
\end{aligned}$$

$$= \frac{E_0}{c}\left[z_0 - z_p\right]\left[a + z_0\right]\left[\left[z_0 - z_p\right]^{-1}\left[\Psi_p^2 + \left[z_0 - z_p\right]^2\right]^{-1/2}\right]$$

$$= \frac{E_0}{c}\left[a + z_0\right]\left[1 - \left[1 + \left[\frac{\Psi_p}{\left[z_0 - z_p\right]}\right]^2\right]^{-1/2}\right]$$

$$E_s = \frac{E_0}{2}\left[z_0 - z_p\right]\left[a + z_0\right]\int_{\left[z_0 - z_p\right]^2}^{\Psi_p^2 + \left[z_0 - z_r\right]^2} \upsilon^{-2} d\upsilon$$

$$= \frac{E_0}{2}\left[z_0 - z_p\right]\left[a + z_0\right]\left[\left[z_0 - z_p\right]^{-2} - \left[\Psi_p^2 + \left[z_0 - z_p\right]^2\right]^{-1}\right]$$

$$= \frac{E_0}{2}\frac{a + z_0}{z_0 - z_p}\left[1 - \left[1 + \left[\frac{\Psi_p}{\left[z_0 - z_p\right]}\right]^2\right]^{-1}\right]$$

$$= \frac{E_0}{2}\frac{a + z_0}{z_0 - z_p}\left[1 + \left[\frac{z_0 - z_p}{\Psi_p}\right]^2\right]^{-1} \tag{4.3}$$

Note that E_s has units V/m, while E_δ has units Vs/m corresponding to the time integral (or area) of the δ function.

5. Some Design Considerations

Summarizing, we have

$$
\begin{aligned}
E_\delta &= \frac{E_0}{c}\left[a+z_0\right]\left[1-\left[1+\left[\frac{\Psi_p}{z_0-z_p}\right]^2\right]^{-1/2}\right] \simeq \frac{V_0}{\pi f_g c}\frac{a+z_0}{a-z_0}\cot\left(\frac{\theta_c}{2}\right)\left[1-\left[1+\left[\frac{\Psi_p}{z_0-z_p}\right]^2\right]^{-1/2}\right] \\
E_s &= \frac{E_0}{2}\frac{a+z_0}{z_0-z_p}\left[1+\left[\frac{z_0-z_p}{\Psi_p}\right]^2\right]^{-1} \simeq \frac{V_0}{2\pi f_g}\frac{1}{z_0-z_p}\frac{a+z_0}{a-z_0}\cot\left(\frac{\theta_c}{2}\right)\left[1+\left[\frac{z_0-z_p}{\Psi_p}\right]^2\right]^{-1} \\
E_p &= \frac{V_0}{2\pi f_g z_0}\tan\left(\frac{\theta_c}{2}\right) \quad , \quad E_p\ \Delta t_p \simeq \frac{V_0}{2\pi f_g c}\frac{a-z_0}{z_0}\tan\left(\frac{\theta_c}{2}\right) \\
E_0 &= \frac{V_0}{\pi f_g}\frac{1}{a=z_0}\cot\left(\frac{\theta_c}{2}\right)
\end{aligned}
\tag{5.1}
$$

One can compute θ_c from z_p (or Ψ_p) in (1.5). For the special symmetric case of $z_p = 0$, merely replace $\Psi_p = b$, giving

$$
\begin{aligned}
E_\delta &= \frac{E_0}{c}\frac{b^2}{a} \simeq \frac{V_0}{\pi f_g c}\frac{b}{a} \quad , \quad E_s = \frac{E_0}{2}\ \frac{a+z_0}{z_0}\ \frac{b^2}{a^2} \simeq \frac{V_0}{2\pi f_g}\frac{a+z_0}{z_0}\frac{b}{a^2} \\
E_p &\simeq \frac{V_0}{2\pi f_g}\frac{a+z_0}{bz_0} \quad , \quad E_p\ \Delta t_p \simeq \frac{V_0}{\pi f_g c}\frac{b}{z_0} \\
E_0 &\simeq \frac{V_0}{\pi f_g b}
\end{aligned}
\tag{5.2}
$$

A first observation concerns the common factor $V_0/(\pi f_g)$. For large fields one needs large voltage and low wave-launcher impedance. Note that an extra factor of $\sqrt{2}$ increase in the fields is obtained by going to a 4-arm feed in the usual sense of a IRA with arms at 45° [4], and a little more can be achieved by arms at about 60° from the horizontal (the *x* = 0 plane) as projected on a constant-z plane [7, 8]. This is just another common factor with which we can deal separately.

The δ-function part of the field does not have infinite amplitude when the incident step-like wave has a nonzero rise time. For simplicity let us imagine that the δ-function is replaced by

$$
\delta(t) \to \frac{1}{t_\delta}\left[u(t)\ -\ u(t-t_\delta)\right] \tag{5.3}
$$

i.e., a gate function of width t_δ and height t_δ^{-1}. This makes the impulsive part of the field have amplitude $E_\delta t_\delta^{-1}$, showing the importance of a small pulse width. For convenience define

$$T \equiv \frac{\Delta t_p}{t_\delta} = \frac{2[a - z_0]}{ct_\delta} \tag{5.4}$$

We will want this to be large, which argues for large *a*.

Considering the simpler case $z_p = 0$ we have

$$\frac{E_s}{E_p} \simeq \frac{b^2}{a^2} < 1 \tag{5.5}$$

If we want the step from the reflector (the post pulse if you like) to cancel the prepulse step then one would like *b* to approach *a*, but this has other consequences. Next compare the main (δ) pulse amplitude to the prepulse amplitude giving

$$\frac{E_\delta}{t_\delta E_p} \simeq 2\frac{b^2 z_0}{act_\delta}[a + z_0]^{-1} = 2\frac{b^2}{a}\frac{T}{ct_p}\frac{z_0}{a + z_0} = \frac{z_0}{a}T \tag{5.6}$$

The factor z_0 / a is less than one, but it needs to be large to give a large main pulse. This is further aided by a large T implying large $a - z_0$ and small t_δ. So, intermediate values of z_0 are called for, i.e., at the maximum of $z_0[a - z_0]$ which is

$$\begin{aligned} z_0 &= \frac{a}{2}, \quad b = \frac{\sqrt{3}}{2}a \\ \theta_c &= \frac{3}{4}\pi = 135^\circ \\ \frac{b^2}{a^2} &= \frac{3}{4} \end{aligned} \tag{5.7}$$

6. Spot Size

Given that the impulse has some small width t_δ, the maximum fields will exist in some small region around $\vec{r}_0$. So let us estimate a pulse width of this impulsive part for positions near $\vec{r}_0$. For the δ-function pulse we have the wave from every position on S_a arriving at exactly the same time at $\vec{r}_0$. We can then estimate a pulse width near $\vec{r}_0$ by the dispersion in the arrival times from all parts of S_a at the observation point.

For this purpose, consider the lengths of the ray paths in Fig. 6.1 indicating the maximum time differences from the edges and center of S_a to the observer. For an observer at $z_0 + \Delta z$ on the z axis we have

$t_c \equiv$ arrival time from center

$ct_c = 2a + \Delta z$

$t_e \equiv$ arrival time from edge

$$
\begin{aligned}
c\,t_e &= \left[\left[z_0 + z_p\right]^2 + \Psi_p^2\right]^{1/2} + \left[\left[z_0 - z_p + \Delta z\right]^2 + \Psi_p^2\right]^{1/2} \\
&\simeq \left[\left[z_0 + z_p\right]^2 + \Psi_p^2\right]^{1/2} + \left[\left[z_0 - z_p\right]^2 + 2\left[z_0 - z_p\right]\Delta z + \Psi_p^2\right]^{1/2} \\
&\simeq \left[\left[z_0 + z_p\right]^2 + \Psi_p^2\right]^{1/2} + \left[\left[z_0 - z_p\right]^2 + \Psi_p^2\right]^{1/2} \left[1 + \frac{\left[z_0 - z_p\right]\Delta z}{\left[\left[z_0 - z_p\right]^2 + \Psi_p^2\right]}\right] \qquad (6.1) \\
&= 2a + \frac{\left[z_0 - z_p\right]\Delta z}{\left[\left[z_0 - z_p\right]^2 + \Psi_p^2\right]^{1/2}}
\end{aligned}
$$

Then we have

$t_z \equiv$ pulse width with respect to $z = \left|t_c - t_e\right|$

$$
ct_z \simeq \left|\frac{z_0 - z_p}{\left[\left[z_0 - z_r\right]^2 + \Psi_p^2\right]^{1/2}} - 1\right|\left|\Delta z\right| \qquad (6.2)
$$

For the special case of $z_p = 0$ we have

$$
ct_z \simeq \left[1 - \frac{z_0}{a}\right]\left|\Delta z\right| \qquad (6.3)
$$

Large z_0 / a (small *b/a*) minimizes this.

For an observer radially displaced $\Delta\Psi$ from $\vec{r}_0$ we have

$t_1 \equiv$ arrival time from near edge

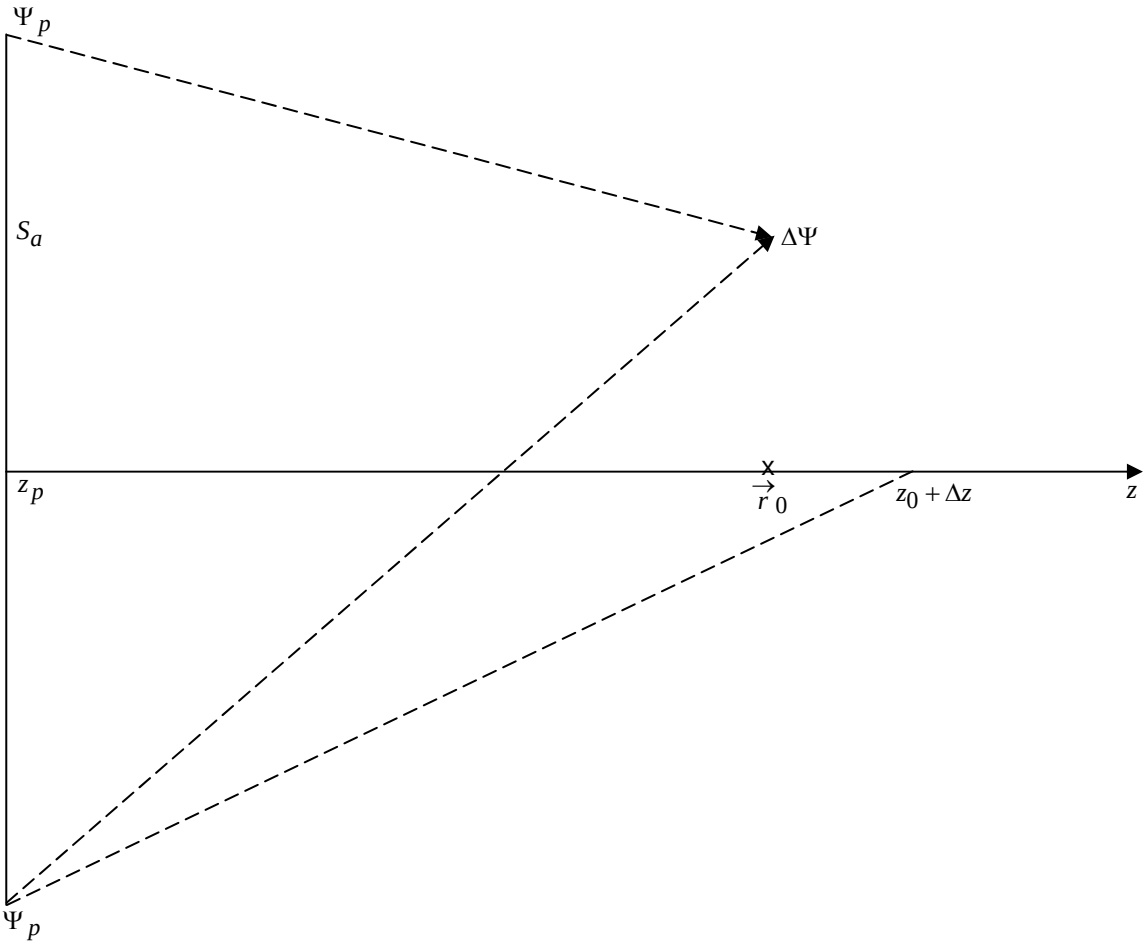

Fig. 6.1 Dispersion of Impulse Near $\vec{r}_0$.

$$
\begin{aligned}
c\,t_1 &= \left[\left[z_0 + z_p\right]^2 + \Psi_p^2\right]^{1/2} + \left[\left[z_0 - z_p\right]^2 + \left[\,\Psi_r - \Delta\Psi\right]^2\right]^{1/2} \\
&\simeq \left[\left[z_0 + z_p\right]^2 + \Psi_p^2\right]^{1/2} + \left[\left[z_0 - z_p\right]^2 + \Psi_p^2 - 2\Psi_p \Delta\,\Psi\right]^{1/2} \\
&\simeq \left[\left[z_0 + z_p\right]^2 + \Psi_p^2\right]^{1/2} + \left[\left[z_0 - z_p\right]^2 + \Psi_p^2\right]^{1/2} \left[1 - \frac{\Psi_r \Delta\Psi}{\left[\left[z_0 - z_p\right]^2 + \Psi_p^2\right]}\right] \\
&= 2a - \frac{\Psi_p \Delta\Psi}{\left[\left[z_0 - z_p\right]^2 + \Psi_p^2\right]^{1/2}}
\end{aligned}
$$

$t_2 \equiv$ arrival time from far edge

$$
ct_2 \simeq 2a + \frac{\Psi_p \Delta\Psi}{\left[\left[z_0 - z_p\right]^2 + \Psi_p^2\right]^{1/2}} \tag{6.4}
$$

Then we have

$t_\Psi \equiv$ pulse width with respect to $\Psi = t_2 - t_1$

$$
ct_\Psi = \frac{2\Psi_p \Delta\Psi}{\left[\left[z_0 - z_p\right]^2 + \Psi_p^2\right]^{1/2}} \tag{6.5}
$$

For the special case of $z_p = 0$ we have

$$
ct_\Psi = 2\frac{b}{a}\Delta\Psi \qquad (\Delta\Psi \text{ positive}) \tag{6.6}
$$

Small *b/a* also minimizes this.

Comparing these pulse widths to t_δ, the width at $\vec{r}_0$, we can note that the pulse widths in the *z* direction are $t_\delta + t_z$, and in the Ψ direction $t_\delta + t_\Psi$. The physical spot size is then given by (counting width in both directions from $\vec{r}_0$)

$$
t_\Psi \simeq t_z \simeq 2\,t_\delta \tag{6.7}
$$

Given by (6.2) and (6.4). For the special case of $z_p = 0$ we have

$$
\left|\Delta z\right| \simeq 2\left[1 - \frac{z_0}{a}\right]^{-1} ct_\delta \quad , \quad \Delta\Psi \simeq \frac{a}{b}\, ct_\delta \tag{6.8}
$$

Of course, these are just rough estimates. Detailed waveform calculations will give more accurate results, including actual waveforms instead of bounds on pulse widths.

7. Concluding Remarks

This modest study has found some analytic approximations useful for estimating the focal waveforms and focal spot size for the prolate-spheroidal IRA. One may think of this as analogous to the first of the papers dealing with the IRA using a paraboloidal reflector [3]. Considering the sophisticated design papers which followed the introduction of the IRA concept, there is much yet to be done for the prolate-spheroidal version.

Here we have found some especially simple results for the case of reflector truncation at $z_p = 0$. More detailed numerical treatment of the results for $z_p \neq 0$ may lead to yet more insight into an optimal design.

References

1. C. E. Baum, “Impedances and Field Distributions for Symmetrical Two Wire and Four Wire Transmission Line Simulators”, Sensor and Simulation Note 27, October 1966.

2. C. E. Baum, “Focused Aperture Antennas”, Sensor and Simulation Note 306, May 1987.

3. C. E. Baum, “Radiation of Impulse-Like Transient Fields”, Sensor and Simulation Note 321, November 1989.

4. C. E. Baum, “Configurations of TEM Feed for an IRA”, Sensor and Simulation Note 327, April 1991.

5. C. E. Baum, “Aperture Efficiencies for IRAs”, Sensor and Simulation Note 328, June 1991.

6. C. E. Baum, “Circular Aperture Antennas in Time Domain”, Sensor and Simulation Note 351, November 1992.

7. C. E. Baum, “Selection of Angles Between Planes of TEM Feed Arms of an IRA”, Sensor and Simulation Note 425, August 1998.

8. J. S. Tyo, “Optimization of the Feed Impedance for an Arbitrary Crossed-Feed-Arm Impulse Radiating Antenna”, Sensor and Simulation Note 438, November 1999.

9. C. E. Baum, “Prodicing Large Transient Electromagnetic Fields in a Small Region: An Electromagnetic Implosion”, Sensor and Simulation Note 501, August 2005.

10. C. E. Baum, “Combining Multiple Prolate Spheroidal Reflectors as a Timed Array with a Common Near-Field Focus”, Sensor and Simulation Note 504, November 2005.

11. C. E. Baum, “Prolate Spheroidal Scatterer for Spherical TEM Waves”, Sensor and Simulation Note 508, January 2006.

12. E. G. Farr and C. E. Baum, “Radiation from Self-Reciprocal Apertures”, ch. 6, pp. 281-308, in C. E. Baum and H. N. Kritikos (eds.), *Electromagnetic Symmetry*, Taylor & Francis, 1995.